Supplementary information

A dual-dimensional fluorescent sensor for uranyl (UO_2^{2+}) in complex waters based on a Tb-MOF with intensity–lifetime dual readouts

Yue Ma,[a] Chang Shi,[d] Xuan Jiang,[c] Tonghuan Liu,[*c] Pingru Su,[*a] and Yu Tang[*a, b]

a. State Key Laboratory of Natural Product Chemistry, Key Laboratory of Nonferrous Metal Chemistry and Resources Utilization of Gansu Province, College of Chemistry and Chemical Engineering, Lanzhou University, Lanzhou, 730000, P. R. China.

b. State Key Laboratory of Baiyunobo Rare Earth Resource Researches and Comprehensive Utilization, Baotou Research Institute of Rare Earths, Baotou 014030, P. R. China

c. Frontier Science Center for Rare Isotopes, School of Nuclear Science and Technology Lanzhou University Lanzhou 730000, P. R. China

d. College of Chemistry and Molecular Engineering, Peking University, Beijing 100871, P. R. China

*Correspondence to be done at: liuth@lzu.edu.cn, supr@lzu.edu.cn, tangyu@lzu.edu.cn

Chemicals and Materials.

Terbium (III) nitrate hexahydrate ($Tb(NO_3)_3 \cdot 5H_2O$) was purchased from HEOWNS, H_2BDC-OH were purchased from Energy Chemical, 2-fluorobenzoic acid were purchased from Bide Pharmatech Co., Ltd., and used without further purification. All chemicals have a purity of over 99% and can be used directly without further purification. All aqueous solutions were prepared using deionized water (DI water).

Instrumentation and Characterization. The powder X-ray diffraction (PXRD) patterns were measured with Cu-Kα radiation ($5° < 2\theta < 50°$) under Rigaku MiniFlex 600. The UV-vis absorption spectra were recorded on UV-2600 220V, CH. The photoluminescence (PL) spectra were collected on a Horiba Instruments FL-3 Fluorescence spectrometer (Side Entrance Slit: 1 nm, Side Exit Slit: 1 nm), and fluorescence decay curves. The scanning electron microscope (SEM) images and energy dispersive spectroscopy (EDS) mapping images were acquired by SU8600 (Hitachi, Japan).

X-ray Crystallography. Single-crystal data were collected on XtaLAB Synergy-DW with an HyPix-6000HE detector using the hotonJet-R X-ray source consists of Mo Kα radiation (λ = 0.71073 Å) at 150 or 293 K. Such single crystal diffractometer consists of dual-wavelength rotating anode X-ray source diffractometer with hybrid pixel array detector and kappa goniometer. The temperature during the test is controlled by the Oxford Cryostream 800. The unit cells and data collections for the crystal of ZJU-168 were determined with Olex2. The structure was solved by direct methods, and refined anisotropically.

BET. N_2 adsorption–desorption isotherms were measured at 77 K using a ASAP2406 instrument. Approximately 300 mg of the sample was were exchanged with acetone 2 times (12 for each exchange) and degassed under vacuum at 120 °C for 12 h prior to analysis. The specific surface area was calculated using the BET method in the relative pressure (P/P_0) range of 0-1. Pore volume and pore size distribution were determined from the adsorption branch using the BJH method.

Synthesis of material

The synthesis of compound ZJU-168 was initially reported.[1] A 2-hydroxyterephthalic acid (H_2BDC-OH, 26.4 mg, 0.145 mmol), $Tb(NO_3)_3 \cdot 6H_2O$ (64.7 mg, 0.145 mmol), 2-fluorobenzoic acid (2-FBA, 162.3 mg, 1.16 mmol), N,N′-dimethylformamide (DMF, 7.3 mL), H_2O (0.6 mL), and HNO_3 (0.2 mL, 3.5 M in DMF) were sealed into a 30 mL Teflon cup. Then, the resulting solution was heated to 110 °C for 3 days and cooled to room temperature. The octahedral crystals were collected and washed with DMF and

ethanol for three times.

Hydrolytic Stability Measurements.

To assess the hydrolytic stability of compound ZJU-168, samples (10 mg) were immersed in aqueous solutions spanning a broad pH range (2, 4, 6, 8, and 10) for a duration of 36 hours under ambient conditions. Then the PXRD patterns of these samples were collected and compared to the simulated PXRD pattern to confirm the hydrolytic stability of ZJU-168.

Luminescence Stability Measurements.

To investigate the luminescence stability of ZJU-168, three sets of experiments were conducted. In the first set, the samples were soaked in aqueous solutions with varying pH values (2, 4, 6, 8, 10, and 12) for a duration of 24 hours. In the second set, the samples were immersed in an aqueous solution with a pH of 7 for different time intervals, namely 1, 2, 3, 4, 5, 6, and 7 days. Subsequently, the luminescence spectra of these samples were collected at an excitation wavelength (λ_{ex}) of 365 nm. In the last set, the sample were immersed in Bohai seawater and Liuxiu Lake water (both adjusted to pH = 4 to match the sensing conditions used in this work) for 24 h. By analyzing the changes in their luminescence intensities, the luminescence stability of ZJU-168 was confirmed.

UO_2^{2+} Detection Experiments.

The crystalline material of compound ZJU-168 was finely ground prior to use. Subsequently, 2 mg of ZJU-168 was dispersed in 2 ml of UO_2^{2+} solutions (pH = 4) with concentration ranging from 0 to 200 μM. The resulting mixtures were subjected to ultrasonic homogenization for approximately 10 minutes to ensure uniform dispersion. After 5 h soaking, the luminescence spectra of these suspensions were collected. To evaluate ionic interference effects, parallel experiments were performed by introducing competing species into the suspensions of ZJU-168. Specifically, 2 mg aliquots of ZJU-168 were separately dispersed in 2 mL of 3.7 mM UO_2^{2+}, K^+, Na^+, Li^+, Cd^{2+}, Mn^{2+}, Ni^{2+} Zn^{2+}, Ca^{2+}, Hg^{2+}, Mg^{2+}, Al^{3+}, Ag^+, Cl^-, Br^-, HCO_3^-, SO_4^{2-} and CO_3^{2-} aqueous solutions, respectively, while maintaining identical pH and contact time parameters. A control experiment containing only distilled water was simultaneously prepared following the same dispersion protocol. After 5 h soaking, the luminescence spectra of these suspensions were collected. To achieve the recycling of the material, ZJU-168 was washed with HNO_3 aqueous solution (pH = 4) for twice. In the mixed ion experiments, the experimental procedure was consistent with that described previously, and the concentration of each mixed ion was fixed at 0.37 mM. It should be noted that, in both seawater and lake water sensing experiments, the collected water samples were first

adjusted to pH = 4 before preparing UO_2^{2+} solutions with different concentrations. Therefore, all sensing measurements reported in this work were conducted under pH = 4 conditions, which are consistent with the stability evaluation conditions.

The Calculation Method

All DFT calculations were performed using Gaussian 16 program. The geometry structures of Lig and UO_2^{2+} were optimized at PBE0-D3 level with def2TZVP basis sets. The wave function analysis were carried out by Multiwfn software and the orbitals were visualized by VMD[2].

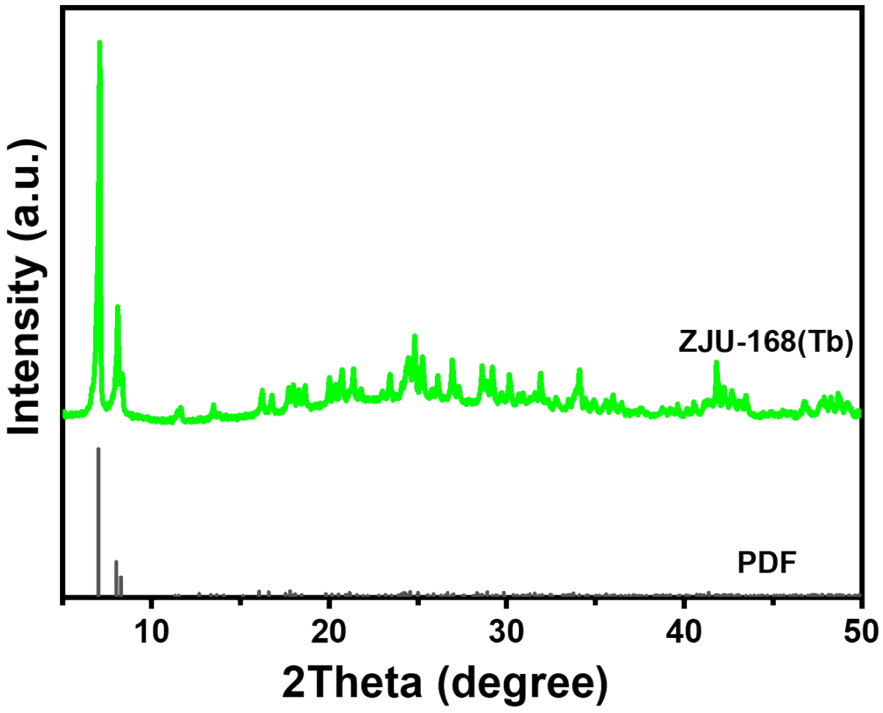

Fig. S1 PXRD pattern of as-synthesized ZJU-168 compared with the simulated one.

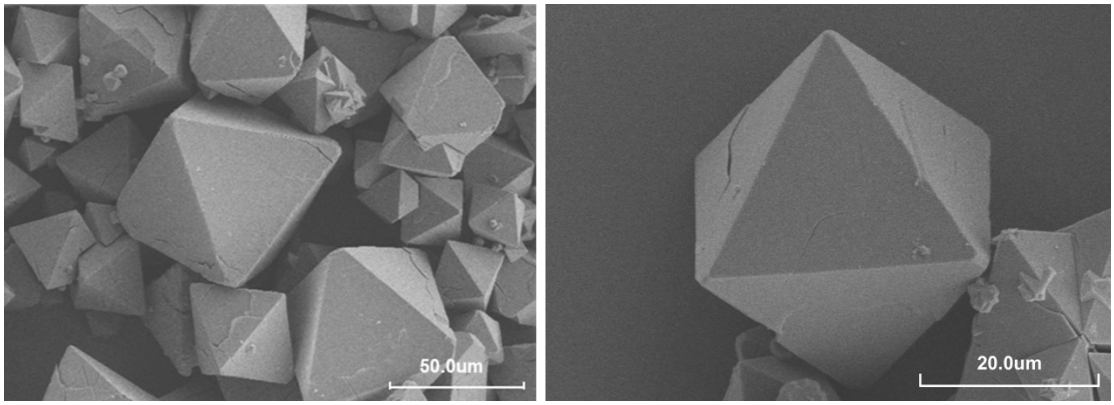

Fig. S2 SEM of ZJU-168.

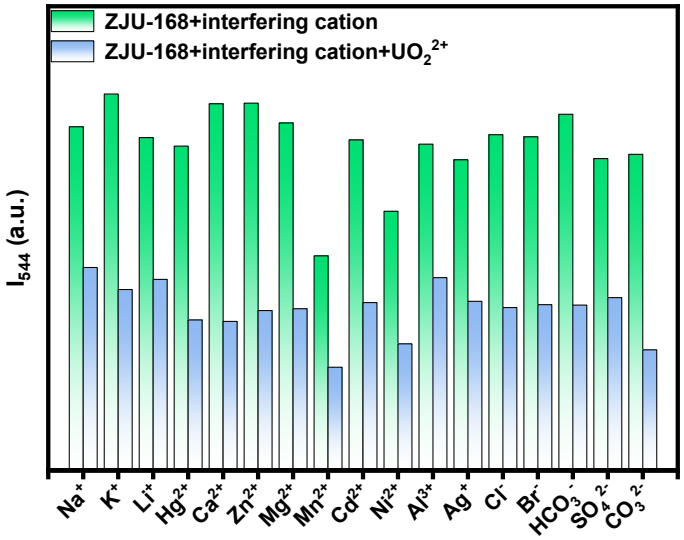

Fig. S3 Fluorescence intensity of ZJU-168 upon addition of UO_2^{2+} in the presence of interfering ions.

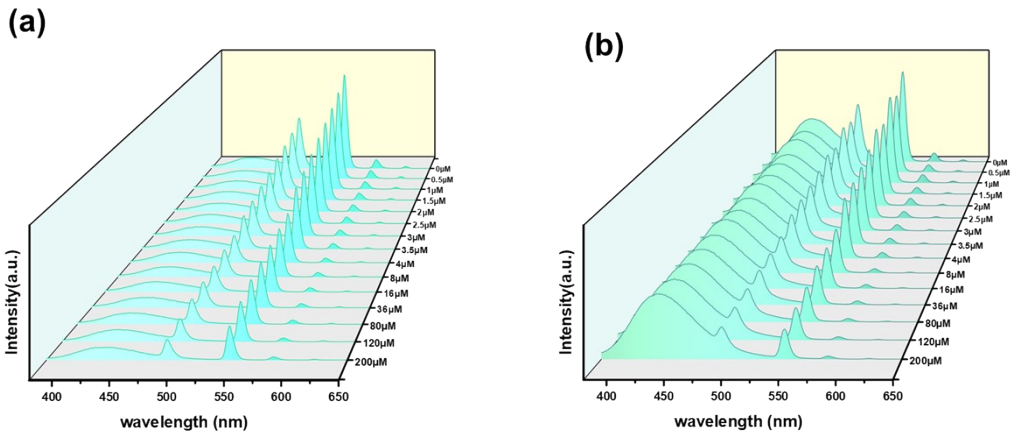

Fig. S4 Fluorescence emission spectra of ZJU-168 upon titration with increasing concentrations of UO_2^{2+} (0–200.0 μM) in (a) lake water and (b) seawater.

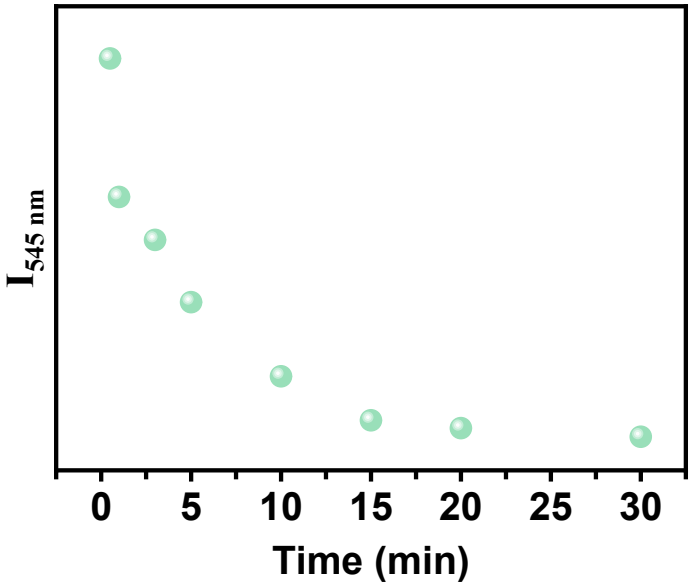

Fig. S5 Fluorescence intensity changes at 545 nm after the addition of UO_2^{2+}.

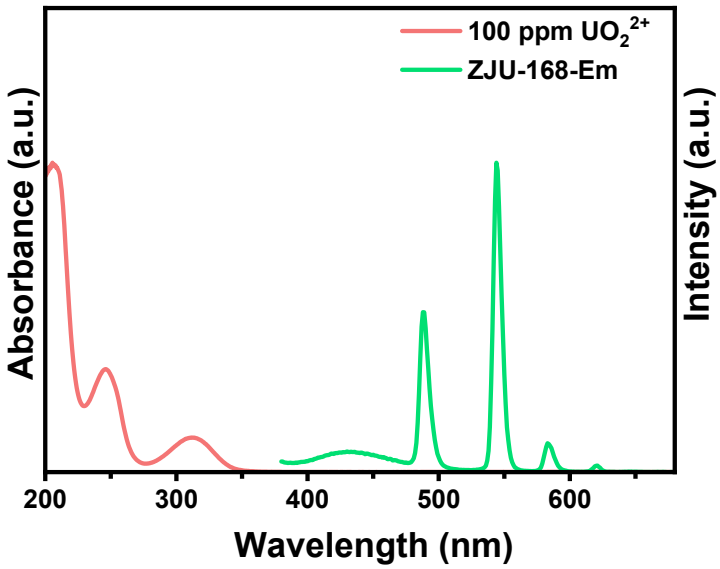

Fig. S6 UV–Vis spectra of uranyl ion solution and fluorescence emission spectra of ZJU-168.

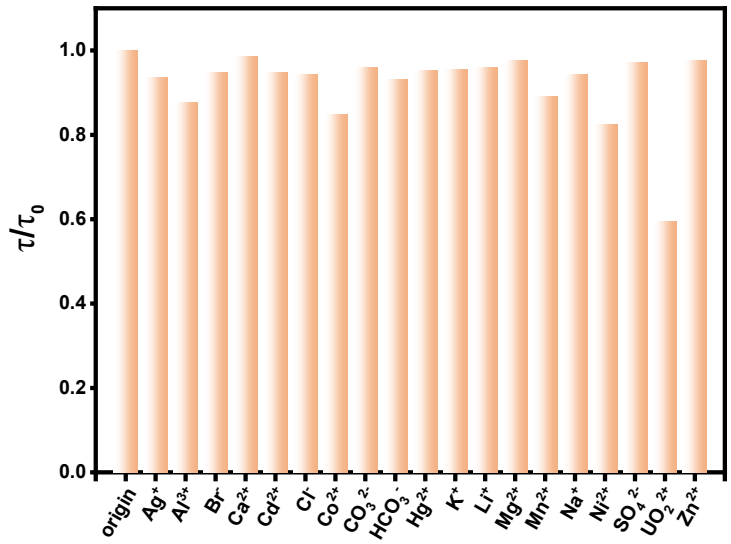

Fig. S7 The corresponding lifetime at 545 nm of ZJU-168 treated with various potential interfering ions.

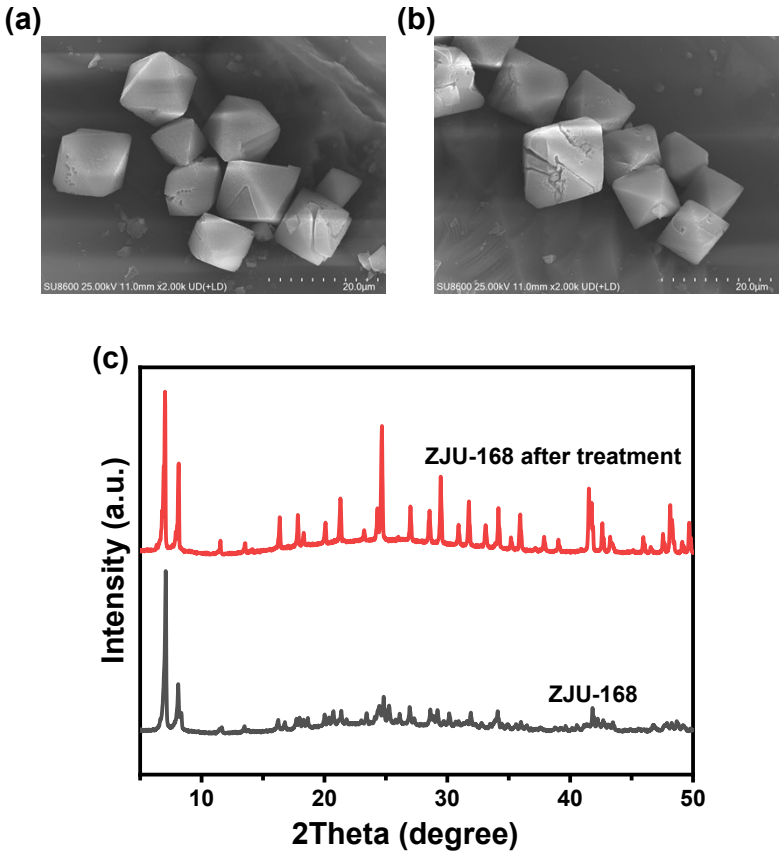

Fig. S8 (a, b) SEM and (c) PXRD after eight washing cycles with HNO_3 (pH = 4) solution.

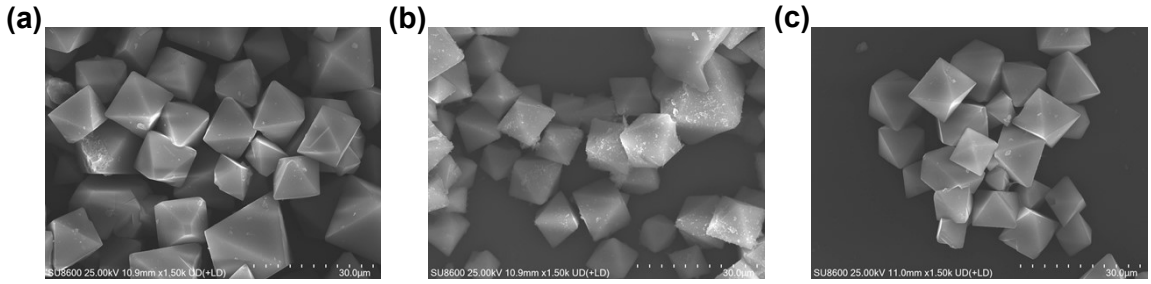

Fig. S9 SEM of ZJU-168 immersed 24 h in (a) 50 ppm UO_2^{2+} solution, (b) seawater and (c) lake water.

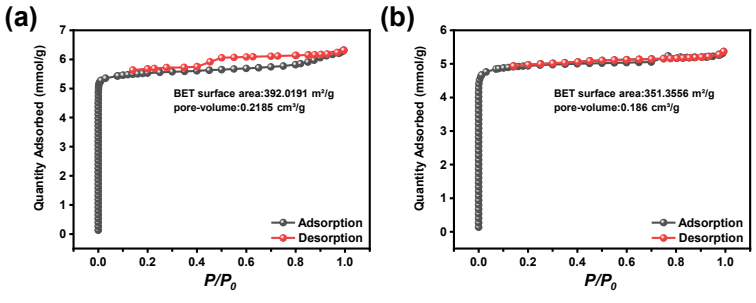

Fig. S10 N_2 adsorption-desorption isotherms at 77 K of (a) ZJU-168 and (b) ZJU-168 after immersion in seawater for 24 h.

Table S1. Fluorescence lifetime of Tb^{3+} at 545 nm (corresponding to the $^5D_4 \rightarrow {}^7F_5$ transition) at different UO_2^{2+} concentrations (0–200.0 μM) in deionized water, lake water, and seawater.

C/uM	$\tau_{544\,nm}$/us		
	Deionized water	Lake water	Sea water
0	707	1090	1229
36	692	830	872
80	659	801	835
120	634	742	786
200	563	654	684

The limit of detection (LOD) for UO_2^{2+} ions was evaluated by the following equations:[3]

$$\sigma = {}^{2}\sqrt{\frac{\sum(\frac{I_0}{I}-1)^2}{N-1}} = 8.76 \times 10^{-4}$$

$$LOD = \frac{3\sigma}{K_{sv}}$$

where σ is the standard deviation for the emission intensities of ZJU-168 immersed in deionized water without UO_2^{2+} ions (N = 11); I_0 is the emission intensity of ZJU-168 in suspension without UO_2^{2+} ions; I is the average value of I_0.

Table S2. Potentiality assessment comparison table for aqueous medium UO_2^{2+} sensing.

MOF	Quenching efficiency Constant (Ksv, M^{-1})	LOD	Ref.
Eu-MOF	8.40×10^{4}	0.9 μM	Anal. Bioanal. Chem. 2019, 411, 4213-4220.
HNU-50	--	1.2×10^{-2} μM	Inorg. Chem. 2020, 59, 9857-9865.
1-Cd	2.70×10^{5}	3.1×10^{-2} μM	Chem. Eur. J. 2021, 27, 16415-16421.
LTP@UiO-66-NH_2	1.81×10^{5}	0.08 μM	Anal. Chem. 2022, 94, 10091-10100.
UiO-66-NH_2	9.94×10^{4}	0.2 μM	
Tb@MOF-808-TDA.	--	5×10^{-3} μM	ACS Appl. Mater. Interfaces 2023, 15, 16882–16894
TOCNF@Eu-MOF	8.21×10^{4}	0.66 μM	Anal. Chim. Acta 2024, 1292, 342211.
Eu-DATP	--	2.7×10^{-3} μM	Anal. Chem. 2024, 96, 7, 3070–3076
Tb@UiO-66-$(COOH)_2$	2.16×10^{5} (in deionized water)	8.03×10^{-3} μM	Inorg. Chem. 2025, 64, 29, 14741–14746
	2.10×10^{5} (in lake water)	8.26×10^{-3} μM	
	3.05×10^{5} (in seawater)	5.68×10^{-3} μM	
Tb-MOF	1.42×10^{5} (in deionized water)	1.39×10^{-2} μM	Inorg. Chem. 2025, 64, 3616–3625
	1.13×10^{5} (in lake water)	1.74×10^{-2} μM	
	1.06×10^{5} (in seawater)	1.86×10^{-2} μM	
This work	1.52×10^{5} (in deionized water)	1.72×10^{-2} μM	
	2.26×10^{5} (in lake water)	1.18×10^{-2} μM	
	1.87×10^{5} (in seawater)	1.41×10^{-2} μM	

References

1. T. Xia, Y. Wan, Y. Li and J. Zhang, *Inorg. Chem.*, 2020, **59**, 8809-8817
2. M. Fu, C. Mao, C. Wei, C. Wang, Q. Kan, S. Dong and L. Mao, *JACS Au*, 2025, **5**, 4044-4054
3. Y.-J. Yang, Y.-H. Li, D. Liu and G.-H. C. Cui, *CrystEngComm*, 2020, **22**, 1166-1175